NANO LETTERS

pubs.acs.org/NanoLett

A Hybrid Nanosensor for TNT Vapor Detection

Alvaro Díaz Aguilar,[†] Erica S. Forzani,[†] Mathew Leright,[†] Francis Tsow,[†] Avi Cagan,[†] Rodrigo A. Iglesias,[†] Larry A. Nagahara,[‡] Islamshah Amlani,[‡] Raymond Tsui,[‡] and N. J. Tao[†,*]

[†]Center for Bioelectronics and Biosensors, Biodesign Institute, and Department of Electrical Engineering, Arizona State University, Tempe, Arizona 85287, [‡]Embedded Systems Research Center, Motorola Laboratories, Tempe, Arizona 85284

ABSTRACT Real-time detection of trace chemicals, such as explosives, in a complex environment containing various interferents has been a difficult challenge. We describe here a hybrid nanosensor based on the electrochemical reduction of TNT and the interaction of the reduction products with conducting polymer nanojunctions in an ionic liquid. The sensor simultaneously measures the electrochemical current from the reduction of TNT and the conductance change of the polymer nanojunction caused from the reduction product. The hybrid detection mechanism, together with the unique selective preconcentration capability of the ionic liquid, provides a selective, fast, and sensitive detection of TNT. The sensor, in its current form, is capable of detecting parts-per-trillion level TNT in the presence of various interferents within a few minutes.

KEYWORDS Nanosensors, explosive detection, nanowires, conducting polymers, hybrid sensors

Despite recent advances, detecting traces of chemicals in a complex environment containing thousands of interferent chemicals and substances remains a difficult task. An important example is the detection of trace amounts of various explosives including TNT.[1] Many sensors and detection methods have been developed, ranging from fluorescence[2−5] and electrochemical sensors[6,7] to ion mobility[8,9] and mass spectrometers.[10,11] One of the most difficult challenges is to discriminate the analytes from various interferents in harsh and variable environments. Another challenge is sample collection, which is particularly important for explosives that have extremely low vapor pressures (e.g., TNT).[12,13] One of the promising approaches is based on electrochemical methods, which detect electrochemical reactions of analytes in an electrolyte. The fact that electrochemical reactions of different analytes take place at different potentials provides selectivity.[14] The hardware of electrochemical sensors is rather simple and can be readily miniaturized, which is suitable for a hand-held device. However, the need of an electrolyte introduces stability issues arising from solvent evaporation and response time problems due to the diffusion of analytes via the electrolyte layer. In addition, the interferent problem is not completely removed because some potential interferents are electrochemically active within the potential range of interest.

In this work we demonstrate a TNT sensor based on an integrated sensor chip consisting of conducting polymer nanojunctions for conductometric detection and electrodes for electrochemical detection (Figure 1). Using a tripotentiostat, we are able to both independently control the two different detection methods, and cooperatively operate them for hybrid detections. In addition to the electrochemical signature of the analyte, the conducting polymer nanojunctions detect the reaction products, which not only add a new dimension to the selectivity but also improve the sensitivity of the integrated device.[15,16] The benefit of "nano" is not just the reduced dimensions but also increased surface-to-volume ratio, which leads to improved response time and sensivity.[20] Another important but less obvious beneficial factor is that the small separation between the nanoelectrodes allows one to measure relatively large transport current through even poorly conductive polymers. The latter benefit is especially important for conducting polymers that often lose conductivity in a medium required for real applications. Furthermore, the sensor chip is coated with a thin layer of ionic liquid which serves as a highly stable electrolyte[17,18] for the electrochemical detection and in the meantime acts as a surprisingly good preconcentrator, as we have found recently.[19] Both sensing elements are integrated into a single silicon chip and the detection circuit is miniaturized, which are highly attractive for a hand-held device. We demonstrate that the sensor allows us to detect TNT traces within minutes in the presence of common interferents.

Each polymer nanojunction was formed by electropolymerization of 3,4-ethylenedioxythiophene (EDOT) monomers (Sigma-Aldrich) to bridge two gold electrodes (WE1 and WE2) separated by a small (60−100 nm) gap on a silicon chip. In order to measure the conduction current through the nanojunction, electrochemical current or leakage current was minimized by coating WE1 and WE2 with Si_3N_4 except for a 10 × 10 μm window. The chip was fabricated using electron beam lithography following procedures described in our previous publication.[20] Poly(ethylenedioxythiophene) (PEDOT)[21] was chosen for TNT detection because its redox

* Corresponding author, njtao@asu.edu.
Received for review: 07/23/2009
Published on Web: 12/30/2009

DOI: 10.1021/nl902382s | *Nano Lett.* **2010,** *10,* 380-384

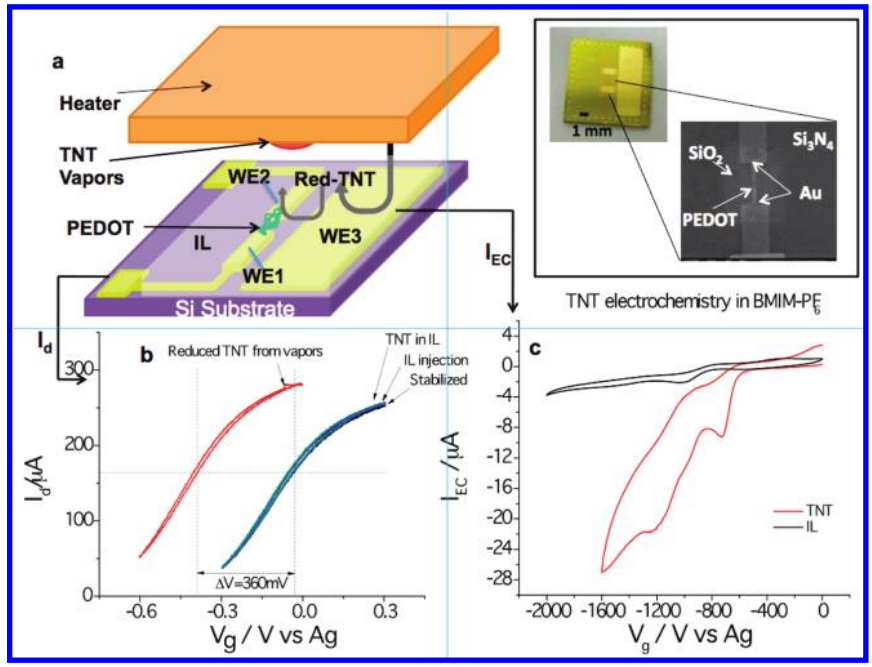

FIGURE 1. (a) A hybrid nanosensor consists of a conducting polymer nanojunction (polymer bridged between WE1 and WE2) and a working electrode (WE3) on a Si chip. The chip is covered with a thin layer of ionic liquid (BMIM-PF_6) serving as electrolyte and preconcentration medium. Upon heating TNT particulates (to 60 °C), TNT vapor is generated which is collected by the ionic liquid layer. The analyte is reduced and detected electrochemically on WE3, and the reduction products are detected by the polymer nanojunctions. Inset: Optical micrograph of the sensor chip used and an SEM image of the PEDOT nanojunction. (b) Current (I_d) via the PEDOT nanojunction plotted as a function of WE1 potential before and after exposure to TNT. (c) Cyclic voltammograms of a blank BMIM-PF_6 solution (black) and 4 ppm TNT in BMIM-PF_6 (red). The large reduction current in the later case is due to the reduction of TNT. Note that a Ag wire quasi-reference electrode and a Pt counter electrode are used (not shown).

response to the reduction products of nitroaromatic compounds (we will return to this latter). The electropolymerization was carried out by cycling the potentials of the two electrodes in 0.1 M EDOT with 1-butyl-3-methylimidazolium hexafluorophosphate (BMIM-PF_6) as supporting electrolyte.[22,23] A Pt wire and a Ag wire were used as a counter electrode and quasi-reference electrode, respectively, and the electrochemical potentials were controlled with a homemade bipotentiostat. During the electropolymerization, a 50 mV bias voltage was applied between WE1 and WE2 while WE1 was cycled between −0.5 and 0.9 V at a rate of 100 mV/s. Successful formation of the polymer nanojunction was confirmed and characterized by measuring the source−drain current (I_d) vs bias (V_{bias}) and I_d vs electrochemical gate voltage (V_g). The former, performed in dry air, exhibits a linear Ohmic relation between −0.1 V and 0.1 V, while the later shows the characteristic redox behavior of PEDOT (Figure 1b).

WE1 or WE2 could not be used as electrodes for electrochemical detection of explosives, for two main reasons: (1) the potential required for the TNT reduction (ca. −1.7 V) irreversibly reduces the polymer destroying its conductivity and (2) both WE1 and WE2 have a relatively small area 15 μm^2, which is not efficient to quickly generate a large quantity of reaction products for the nanojunction sensor. In order to optimize the detection with the nanojunction sensor, a third working electrode (WE3) was fabricated near the polymer nanojunction. WE3 is also made of Au (180 nm thick on 5 nm Cr layer) with an area of 24 mm^2. The surface area of WE3 is 1.6×10^6 times greater than both the areas of WE1 and WE2. WE3 was ∼300 μm away from the nearest nanojunction built on WE1 and WE2. All three working electrodes, WE1, WE2, and WE3, were wire bound to a package and connected to a homemade tripotentiostat for simultaneously monitoring the conductance of the polymer nanojunction formed between WE1 and WE2 and the electrochemical reactions taking place on WE3. This chip design and control are necessary for TNT trace detection, which are different from the two working electrode chips developed by us previously.

Since TNT has an extremely low vapor pressure (4.8×10^{-6} Torr) at room temperature,[13] TNT residues are expected to last for a long time under ambient conditions, which can be collected and detected in vapor form upon heating. To simulate this scenario, a small amount of TNT (e.g., 1−100 μg) was placed on the heating element either directly from the powders or by drying out a TNT solution in acetonitrile (see Supporting Information for more details). TNT vapor was generated by heating the solid residue at 60 °C (Figure 1a).

Before exposure to the TNT vapor, the electrical response of the PEDOT nanojunction was characterized in the ionic liquid by sweeping WE1 potential between −0.3 and 0.3 V

DOI: 10.1021/nl902382s | *Nano Lett.* **2010,** *10,* 380-384

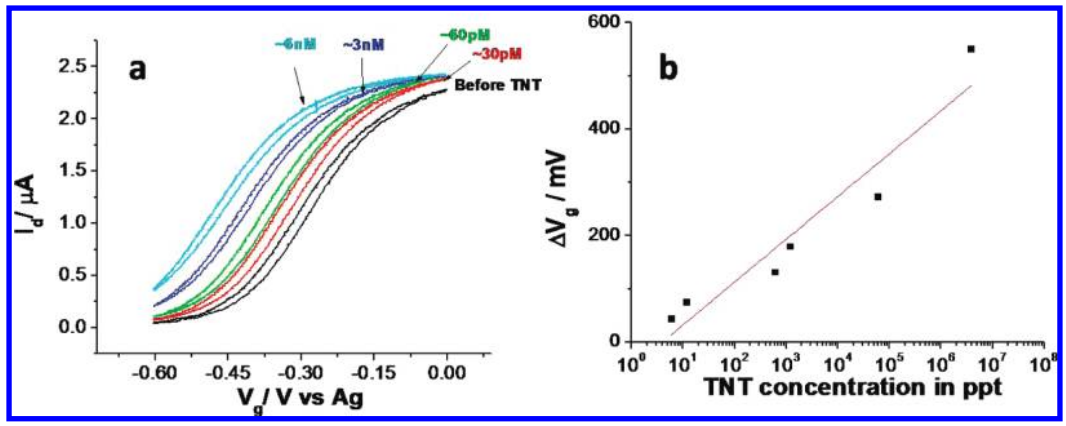

FIGURE 2. (a) I_d-V_g curves for a sensor before TNT exposure (black) and after exposures to solutions with TNT concentrations of 30 pM (red), 60 pM (green), 3 nM (blue), and 6 nM (cyan). (b) The shift of the I_d-V_g (ΔV_g) vs TNT concentration. To cover the wide dynamic ranges the calibration curve was obtained from three different sensors.

with a fixed 50 mV bias between WE1 and WE2. The fixed WE1−WE2 bias was used to drive an electrical current through the nanojunction, and WE1 potential with respect to the reference electrode controls the redox state of PEDOT. As shown in Figure 1b the current via the nanojunction increases with the potential. This is expected because PEDOT transforms from the insulating reduced state at low potentials to the conducting oxidized state at high potentials. The conduction current (I_d) vs potential (V_g) characteristic is rather stable upon repeated sweep of the potential in TNT-free environment. The cyclic voltammogram of the electrolyte solution using WE3 on the same chip shows essentially featureless cyclic voltammograms except for a small broad peak near −1 V (black curve in Figure 1c), due to oxygen reduction in the ionic liquid.[23,24]

Upon exposure to the TNT vapor with no potential applied to WE3, I_d-V_g characteristic of the PEDOT nanojunction remains unchanged (cyan curve in Figure 1b). In contrast, when a negative enough potential (−1.8 to −1.2 V) is applied to the electrode, the cyclic voltammogram (red curve in Figure 1c) shows multiple peaks, due to the reduction of TNT. These distinctive reduction peaks are in good agreement with the findings reported previously (after correction of potential shift due to the use of different reference electrodes).[14,7] This electrochemical response was accompanied by a negative shift in the I_d-V_g curve of the nanojunction. The total amount of the potential shift reached ca. − 0.36 V within 2 min (red curve in Figure 1b), which provides a sensitive detection of TNT. The large response of the PEDOT nanojunction is attributed to the reduction products of TNT that change the redox state of PEDOT, as we will discuss later. The response is limited by the diffusion of the reduction products from WE3 to the PEDOT nanojunction. With mechanical stirring of the ionic liquid, a faster response was observed (Figure S1 in Supporting Information). The fact that the PEDOT nanojunction is sensitive only to the reduction products of TNT is essential for one to discriminate TNT from potential electrochemical active interferents.

The amount of TNT vapor reaching the ionic liquid was estimated with a tuning fork sensor operated as a microbalance.[25,26,19] The surface of the tuning fork sensor is SiO_2 on which TNT vapor is known to stick strongly, allowing us to estimate the TNT vapor flux from the heating element (Supporting Information). In the example discussed above, the estimated concentration was ∼1.7 μM after 3 min of heating the sample.

The response of the PEDOT nanojunction to the reaction products of TNT at different concentrations was studied. Figure 2a shows the results of a sensor chip with TNT concentration varying from 30 pM to 6 nM of TNT in the ionic liquid, which demonstrates that 30 pM (6 parts-per-trillion (ppt)) can be detected with the nanojunction. To examine the dynamic ranges, TNT concentrations up to 1.7 mM were tested, and a calibration plot of the PEDOT nanojunction response vs TNT concentration was obtained (Figure 2b). The plot shows a detection limit of a few ppt with a dynamic range covering at least 6 orders of magnitude of concentrations. This detection limit is significantly better than that of electrochemical method alone and useful for many applications. As we have mentioned earlier, the slow diffusion of the reduction products is currently a factor that limits the sensitivity and response time of the sensor, which can be further improved by optimizing the electrode geometry and the ionic liquid layer thickness. We note that the detection limit was given in terms of concentration in the liquid phase. In terms of vapor concentration, it can be several orders of magnitude lower due to the large preconcentration capability of the ionic liquid (if assuming thermal equilibrium). Another way to describe the detection limit is the total mass of TNT particulates, which is found to be few nanograms (Figure S-3 in Supporting Information). This description is often more practical because TNT has a very low vapor pressure and often collected in the form of particulates.

We have carried out several control experiments in order to confirm that the observed response of the PEDOT nano-

DOI: 10.1021/nl902382s | *Nano Lett.* **2010,** *10,* 380-384

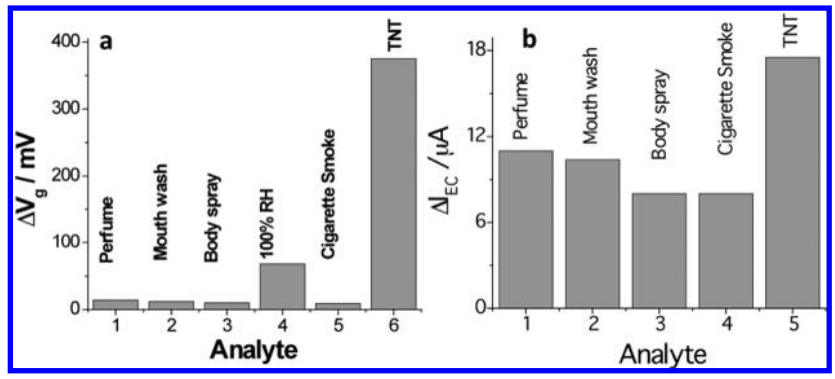

FIGURE 3. Responses of the hybrid nanosensor to different interferents and TNT. (a) ΔV_g is the shift of the I_d vs V_g curve of the PEDOT nanojunction. (a) ΔI_{EC} is the electrochemical reduction current measured by WE3 at −1.2 V.

junction was indeed due to the reduction products of TNT. First, in the absence of TNT, holding WE3 at negative potentials did not result in any response in the PEDOT nanojunction sensor (blue curve on Figure 1b). Second, we added TNT to the ionic liquid (~1.7 μM) but without applying a negative potential to WE3 to reduce TNT, which did not change the response of the nanojunction sensor either (cyan curve on Figure 1b). Finally, we examined possible heating effect on the polymer nanojunction and electrochemical detection during the process of TNT vapor generation. This was done by repeatedly ramping a blank heating element to 60 °C and holding the temperature for a few minutes. In each test, no visible response in the PEDOT nanojunction was observed (see Figure S2 in Supporting Information). These tests also show that the heating does not result in evaporation of the ionic liquid, due to its low vapor pressure and high boiling point.[27]

A useful sensor must be able to discriminate analytes from common interferents in ambient environment. We performed further experiments testing the response of the hybrid nanosensor to different interferents. Figure 3a shows a comparative plot of the potential changes in a PEDOT nanojunction resulting from exposures to a 2% of the saturated vapors of perfume, mouth wash, body spray, and 100% cigarette smoke and as well as TNT vapors. The response of the nanojunction to each of the highly concentrated interferents is negligible comparing to the large shift by the trace level TNT (see raw data in Figure S4, Supporting Information). We have also tested the scenario of a large variation in relative humidity. A high fixed humidity does not affect the detection of TNT, but a large change in humidity can cause a small shift in the I_d-V_g curve of the sensor. For example, increasing the relative humidity (RH) from 50% to 100% can shift the curve by 50 mV. Apparently, although the ionic liquid is hydrophobic, $BMIM^+$ has an acidic C_2-H group and a small amount of water can still dissolve in it due to favorable hydrogen bond interactions.[28] The corresponding shifts for each RH case are plotted versus the RH in Figure S5 (Supporting Information). The humidity effect may be compensated by monitoring the humidity level or reduced by controlling the humidity. However, we note that even at 100% humidity, a few hundred of ppt can still be detected.

We have also compared the effects of the same interferents on the electrochemical detection (Figure 3b). We found that the electrochemical detection alone is more prone to interferents, which underscores the importance of the integrated nanojunction and electrochemical sensor on the same chip. The improved selectivity of the integrated sensor for detection of nitroaromatic molecules can be attributed to (1) the distinct electrochemical signatures given by the specific potentials of the reduction peaks of the nitro groups in nitroaromatic compounds, (2) the strong redox interactions between the reduction products of nitroaromatic compounds and PEDOT (see discussion below), and (3) selective preconcentration of nitroaromatic compounds by the ionic liquid.[19]

A shift in the I_d-V_g curve could be due to either a change in the polymer material[29] in the nanojunction or a potential shift in the reference electrode.[30] In order to determine the origin of the observed potential shift, we monitored the peak positions of TNT reduction reactions using a redox probe (ferrocene) as an internal reference calibration. We found that the exposure of the Ag reference electrode to the TNT reduction products did not cause significant potential shifts in the TNT reduction and ferrocene redox peaks, indicating that the shift in the I_d-V_g curve is not due to changes in the reference electrode. Instead, the shift must be due to the interaction of the TNT reduction products with the PEDOT nanojunction.

We characterized the TNT reduction products using Fourier transform infrared (FTIR) spectroscopy, High-performance liquid chromatography (HPLC) followed by mass spectrometry.[19] The results show the presence of high molecular weight products, such as azo- and azoxy-aromatic dimers, trimers and larger molecules.[19,28,31] To examine if these reduction products can chemically react with the PEDOT nanojunction, we measured the redox reactions of PEDOT via cyclic voltammetry in the presence of the TNT reduction products and found no obvious change in the PEDOT redox reactions. This observation

DOI: 10.1021/nl902382s | *Nano Lett.* **2010,** *10,* 380-384

indicates chemical reactions of the TNT reduction products with the PEDOT are unlikely. However, the negative shift of the I_d-V_g curve produced by the TNT reduction products indicates an interaction between the products and the PEDOT, in which the TNT products act as dopants of the polymer.

In summary, we have demonstrated an integrated electrochemical and electrical nanosensor for sensitive and selective detection of nitroaromatic explosives vapors. The sensor utilizes both the electrochemical signatures of the reduction of the analytes and specific interactions of the reduction products with the polymer nanojunction to achieve excellent selectivity. The electrical detection of the polymer nanojunctions leads to high sensitivity. Furthermore, BMIM-PF_6 is used not only as a stable electrolyte but also as a preconcentration medium for nitroaromatic compounds. The sensor is capable of detecting ppt-level TNT within 1−2 min in the presence of various common interferents found in ambient air. We believe that the integrated sensor can be further optimized and developed into an inexpensive portable device for detection of explosives and the integrated approach that includes multiple coupled detection mechanisms and built-in preconcentration will also be useful for other chemical and biosensors.

Acknowledgment. We thank Joseph Wang and Kevin Linker for their insightful discussions, Jinghong Li for providing us with purified ionic liquid, Christopher Madden for his help in UV−vis spectroscopy and electrochemical studies, and NSF for partial support.

Supporting Information Available. Detailed information on TNT vapor generation, diffusion of reaction products, thermal stability of the polymer nanojunctions, TNT concentrations from vapor generation, interference studies, and humidity effects. This material is available free of charge via the Internet at http://pubs.acs.org.

REFERENCES AND NOTES

(1) Nambayah, M.; Quickenden, T. I. *Talanta* **2004**, *63* (2), 461–467.
(2) Naddo, T.; Yang, X. M.; Moore, J. S.; Zang, L. *Sens. Actuators, B* **2008**, *134* (1), 287–291.
(3) Albert, K. J.; Walt, D. R. *Anal. Chem.* **2000**, *72* (9), 1947–1955.
(4) Cumming, C. J.; Aker, C.; Fisher, M.; Fox, M.; la Grone, M. J.; Reust, D.; Rockley, M. G.; Swager, T. M.; Towers, E.; Williams, V. *IEEE Trans. Geosci. Remote Sensing* **2001***39* (6), 1119–1128.
(5) Hughes, A. D.; Glenn, I. C.; Patrick, A. D.; Ellington, A.; Anslyn, E. V. *Chem.—Eur. J.* **2008**, *14* (6), 1822–1827.
(6) Wang, J. *Electroanalysis* **2007**, *19* (4), 415–423.
(7) Zhang, H. X.; Cao, A. M.; Hu, J. S.; Wan, L. J.; Lee, S. T. *Anal. Chem.* **2006**, *78* (6), 1967–1971.
(8) Reid Asbury, G.; Klasmeier, J.; Hill, H. H., Jr. *Talanta* **2000**, *50* (6), 1291–1298.
(9) Ewing, R. G.; Atkinson, D. A.; Eiceman, G. A.; Ewing, G. J. *Talanta* **2001**, *54* (3), 515–529.
(10) Mathurin, J.; Faye, T.; Brunot, A.; Tabet, J. C.; Wells, G.; Fuche, C. *Anal. Chem.* **2000**, *72*, 5055–5062.
(11) Asano, K. G.; Goeringer, D. E.; McLuckey, S. A. *Anal. Chem.* **1995**, *67*, 2739–2742.
(12) Moore, D. S. *Rev. Sci. Instrum.* **2004**, *75* (8), 2499–2512.
(13) Senesac, L.; Thundat, T. G. *Mater. Today* **2008**, *11* (3), 28–36.
(14) Wang, J.; Thongngamdee, S. *Anal. Chim. Acta* **2003**, *485* (2), 139–144.
(15) Ali, S. R.; Ma, Y. F.; Parajuli, R. R.; Balogun, Y.; Lai, W. Y. C.; He, H. X. *Anal. Chem.* **2007**, *79* (6), 2583–2587.
(16) Ramanathan, K.; Bangar, M. A.; Yun, M. H.; Chen, W. F.; Mulchandani, A.; Myung, N. V. *Nano Lett.* **2004**, *4* (7), 1237–1239.
(17) Noda, A.; Susan, A. B.; Kudo, K.; Mitsushima, S.; Hayamizu, K.; Watanabe, M. *J. Phys. Chem. B* **2003**, *107* (17), 4024–4033.
(18) Buzzeo, M. C.; Hardacre, C.; Compton, R. G. *Anal. Chem.* **2004**, *76* (15), 4583–4588.
(19) Forzani, E. S.; Lu, D.; Leright, M. J.; Aguilar, A. D.; Tsow, F.; Iglesias, R. A.; Zhang, Q.; Lu, J.; Li, J.; Tao, N. *J. Am. Chem. Soc.* **2009**, *131* (4), 1390–1391.
(20) Aguilar, A. D.; Forzani, E. S.; Nagahara, L. A.; Amlani, I.; Tsui, R.; Tao, N. J. *Sens. J., IEEE* **2008**, *8* (3), 269–273.
(21) Roncali, J.; Blanchard, P.; Frere, P. *J. Mater. Chem.* **2005**, *15* (16), 1589–1610.
(22) Li, Z. Y.; Liu, H. T.; Liu, Y.; He, P.; Li, J. H. *J. Phys. Chem. B* **2004**, *108* (45), 17512–17518.
(23) Buzzeo, M. C.; Evans, R. G.; Compton, R. G. *ChemPhysChem* **2004**, *5* (8), 1106–1120.
(24) Buzzeo, M. C.; Klymenko, O. V.; Wadhawan, J. D.; Hardacre, C.; Seddon, K. R.; Compton, R. G. *J. Phys. Chem. A* **2003**, *107* (42), 8872–8878.
(25) Ren, M. H.; Forzani, E. S.; Tao, N. J. *Anal. Chem.* **2005**, *77* (9), 2700–2707.
(26) Ren, M. H.; Tsow, T.; Forzani, E. S.; Tao, N. J. *Abstracts of Papers*, 229th National Meeting of the American Chemical Society, San Diego, CA; American Chemical Society: Washington, DC, 2005; U152.
(27) Anderson, J. L.; Armstrong, D. W.; Wei, G. T. *Anal. Chem.* **2006**, *78* (9), 2892–2902.
(28) Hapiot, P.; Lagrost, C. *Chem. Rev.* **2008**, *108* (7), 2238–2264.
(29) Dall'Antonia, L. H.; Vidotti, M. E.; de Torresi, S. I. C.; Torresi, R. M. *Electroanalysis* **2002**, *14* (22), 1577–1586.
(30) Larrimore, L.; Nad, S.; Zhou, X.; Abruna, H.; McEuen, P. L. *Nano Lett.* **2006**, *6* (7), 1329–1333.
(31) Steudel, E.; Posdorfer, J.; Schindler, R. N. *Electrochim. Acta* **1995**, *40*, 1587.

DOI: 10.1021/nl902382s | *Nano Lett.* **2010,** *10,* 380-384